# Biomechanical Accident Investigation Methodology Using Analytical Techniques

D. H. Robbins, J. W. Melvin, D. F. Huelke, and H. W. Sherman University of Michigan Transportation Research Institute

#### **ABSTRACT**

The purpose of this paper is to describe a combination of state-of-the-art detailed acciprocedures, dent investigation computerized and occupant modeling, and vehicle crash biomechanical analysis of human injury causation into a method for obtaining enhanced biomechanical data from car crashes. Four accident cases, out of eighteen investigated, were selected for detailed reconstruction. Three were frontal impacts while the fourth was lateral. The CRASH II and MVMA 2-D analytical models were used in the reconstruction process. Occupant motions, force interactions with vehicle components, accelerations on the various body segments, and much other information was produced in the simulation process and is reported in this paper along with scene and injury data from the accidents. The major conclusion reached was that the reconstructions, using largely preliminary data for the occupant and vehicle, evaluated and the dynamic loadings predicted for application to the car occupants yielded injury results which were generally within accepted ranges of human tolerance data. Additional conclusions were reached about the quality of data describing the occupant, car, and needed for analytical reconstruction.

THE PURPOSE OF THIS PROJECT was to combine presently available advanced computer modeling techniques for reconstructing a crash sequence for application to the development of methods for determining occupant contact velocities, impact forces and occupant responses in passenger car accidents. This preliminary study is intended to develop a methodology to analyze realworld car crashes and to investigate the applicability of computerized vehicle crash and occupant motion simulation modeling techniques to the improvement of accident investigation-based biomechanics data and staged laboratory collision tests.

## BACKGROUND AND METHODS

Ongoing field accident investigations in University of Michigan area have had the potential to incorporate biomechanically specialized additions and to provide for additional accident injury and anthropometric investigations. In Europe this type of detailed investigation has been supplemented by actual staged crash tests with dummies and cadavers to obtain biomechanical human tolerance data. This approach is relatively costly and only a limited number of tests have been performed. In the current project computer simulations were substituted for both the vehicle crash and the occupant motion phases of the study. This approach was expected to be more flexible in studying the variables associated with the cases, less costly, and ultimately of much greater general utility in advancing knowledge of injury causation, human tolerance and protection of occupants in crashes.

The following criteria were the primary factors in choosing an accident for in-depth investigation:

- Occupant injuries of particular biomechanical significance
- 2. Type (direction) of impact
- Reconstructibility of the crash in terms of vehicle factors and kinematics
- Comparability to accidents representative of national accident statistics.

The focus of the project was to detail:

1. the injuries; 2. the contacts producing injury, and; 3. the occupant kinematics responsible for the injury-producing contact. Since injuries were the primary concern, initial identification of a prospective case was by the specific types of injuries sustained in a potentially reconstructible crash. Following this notification, the vehicle and the accident site were investigated in a detailed manner. Based on the medical, vehicle and accident site factors, a review of the case was made. With the detailed medical and vehicle information available in all crashes, case selection was based on

the probability of accurate crash and occupant kinematic reconstruction.

Following the gathering of the accident data, reconstruction of the vehicle crash factors (using the CRASH II computer model) provided a simulation of the vehicle crash with the resulting dynamic data available as input for two- or three-dimensional dynamic occupant motion computer simulation models. The MVMA 2-D occupant motion simulation (1)\* was used in this study. The computerized reconstruction of the occupant kinematics and impact areas was compared with the case data and judgements made as to the realism of the simulation.

## PRELIMINARY CASE INVESTIGATIONS

Eighteen crashes were identified as being of possible interest through the screening of ongoing crash investigations. The preliminary accident data were reviewed and, in some cases, the team inspected the vehicles and the crash scene, before coming to a decision in regard to the utility of the crash. Four of the eighteen cases were judged to have sufficient merit for full reconstruction. The reasons for rejection of the other fourteen are:

- Vehicle motions cannot be handled by CRASH !! (4 cases)
- Minor or no occupant injury (4 cases)
- Vehicle positions not correctly recorded by police (4 cases)
- Crash not representative of national accident statistics (1 case)
- Vehicle damage modified in extraction of occupants (1 case)
- Post-crash position of vehicles unknown (3 cases)
- Fatal injuries. No medical data available (1 case)

 Vehicle not available for crush measurements (1 case)

## DESCRIPTION OF SELECTED CASES

CASE NO. 1: 1981 MERCURY LYNX (FRONTAL IMPACT) - A 1981 Mercury Lynx (35-year-old male unrestrained driver) struck the rear of a 1972 Chevrolet Nova which was stopped on the paved right shoulder of the expressway. Figure 1 is a schematic of the accident scene showing the direct rear-end impact as well as the well-defined resting points of the vehicles. Figure 2 shows the damage to the front end of the Lynx.

The driver was estimated to have continued forward at impact and struck the left sunvisor and header with his forehead, the windshield with his face, the steering wheel with his throat and chest, and the lower panel with his knees.

Interior damage to vehicle the moderate. Briver contact deformed the left sunvisor and contiquous windshield header. After the windshield was starred, continued travel caused a jagged tear in the laminate of about 20 cm (7.87 in.) and an outward bulge of 4 cm (1.57 in.). Chest contact with the steering wheel caused the rim spokes to fold around the hub and forward nearly to the instrument cluster eyebrow. The vehicle steering column was configured to include a V-joint flexible coupling and the right shear capsule was separated about 35 mm (1.38 in.). There was obvious upward rotation and lateral right movement of the Although they did not appear to be column. damaged, the driver may have had his left hand between the steering wheel rim and the two control levers on the left of the steering column or the left side of the instrument cluster eyebrow. The left end of the lower panel below the headlight switch was deformed by the driver's left knee while his right knee deformed the lower panel to the right of the right shear

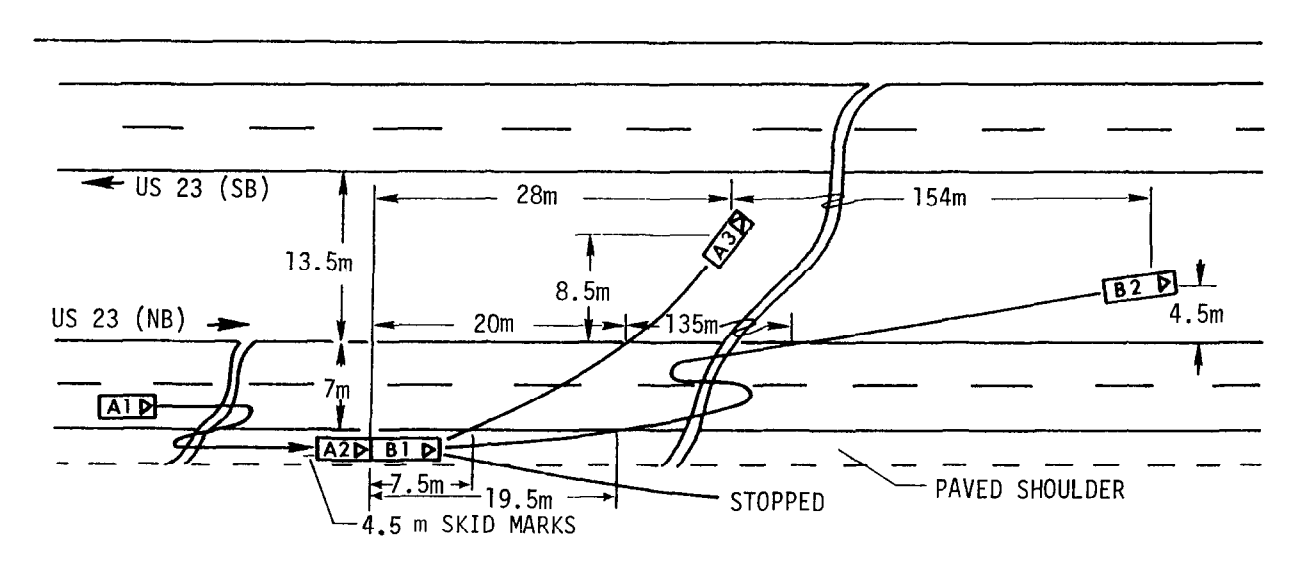


Figure 1. Schematic of Accident Scene (Case No. 1).

<sup>\*</sup>Numbers in parenthesis designate references at the end of paper.

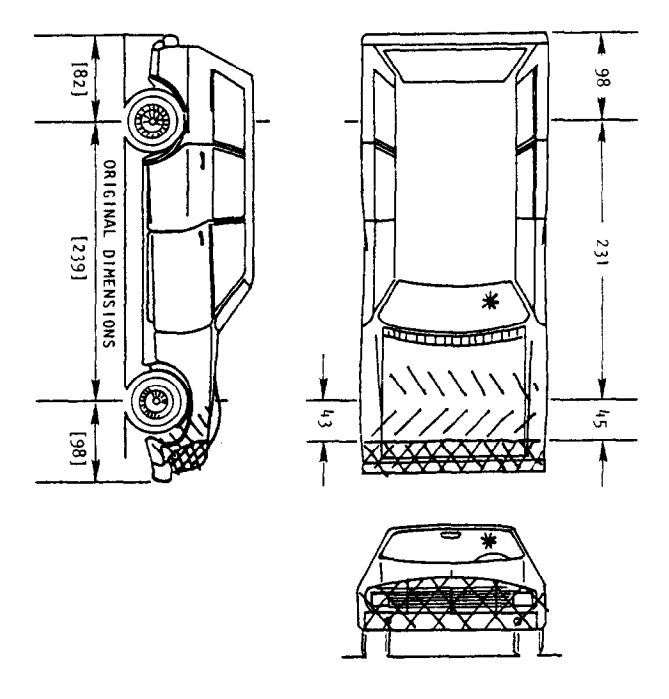


Figure 2. Vehicle Damage (Case No. 1).

capsule location.

The unrestrained driver sustained a variety of injuries during contact with the vehicle interior which were concentrated on the upper chest, neck, and head as defined in Figure 3.

Use of the CRASH II program yielded a velocity change of 22.9 mph (36.9 km/hr) along the axis of the Lynx. This was represented as an acceleration in the form of a trapezoid with a total duration of 80 milliseconds and rise and decay times of 5 milliseconds.

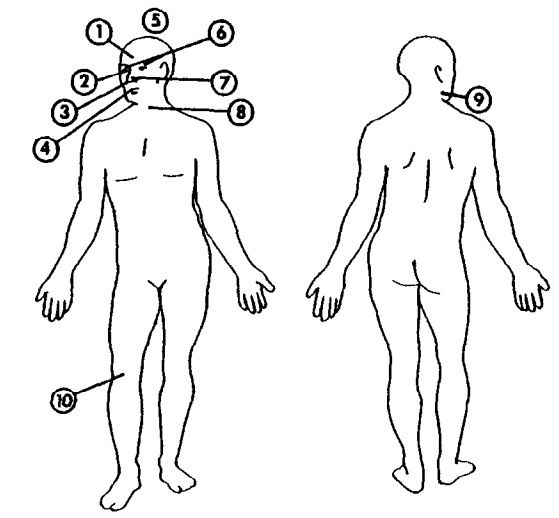
CASE NO. 2: 1977 OLDSMOBILE CUTLASS (FRON-TAL POLE IMPACT) The 1977 Oldsmobile Cutlass S was forced off the roadway and struck a 56 cm diameter tree directly head-on. Frontal crush of the car was 36.6 in. (93 cm). Figure 4 is a schematic of the accident showing the welldefined vehicle motions. Figure 5 shows the severe and almost perfectly symmetric damage sustained by the vehicle.

The unrestrained male driver moved forward and upward after the impact and contacted the sunvisor, header, and windshield with his forehead: the steering wheel rim with his throat; the steering wheel rim and spokes with his chest; the lower panel with his knees; and possibly the mid panel with his right shoulder and forearm.

Interior damage to the vehicle was moderate. The left sunvisor and header were damaged and the windshield was starred by the driver. The lower half of the steering wheel rim was severely bent and the spokes were slightly deformed. The energy absorbing device was compressed about 123 mm (4.84 in.) and the shear capsules were separated. Driver knee impact broke the mid and lower panel areas to both the left and right of the steering column.

The unrestrained driver sustained injuries

- 1. Abr. Rt. Forehead (1)\*
- 2. Abr Rt. Cornea (1)
- 3. 2 cm. Lac. Rt. Nostril (1) 4. 6 cm. Vent. T & T Lac.
- Rt. Upper Lip (1)
- 5. Unconscious (2-3 min.) (2) 6. Abrs. Both Eyelids (1)
- 7. Abr. Nose (1)
- 8. Possible Fx. Larynx with pneumolarynx and hemorrhage Rt. Vocal Cord (4)
- 9. Abr. Rt. Jaw (1)
- 10. Cont. and Abr. Rt. Knee (1)



\*Number in parenthesis is the estimated AIS number.

- 1. Cracked Sternum (2)
- 2. Comminuted Fxs. Proximal and mid portion 4th and 5th Lt. Metacarpals (2)

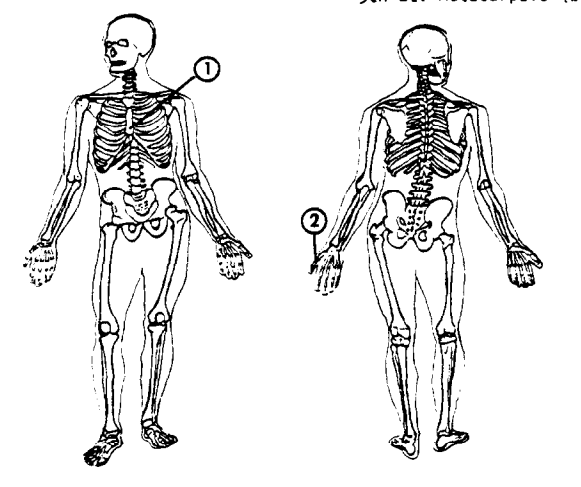
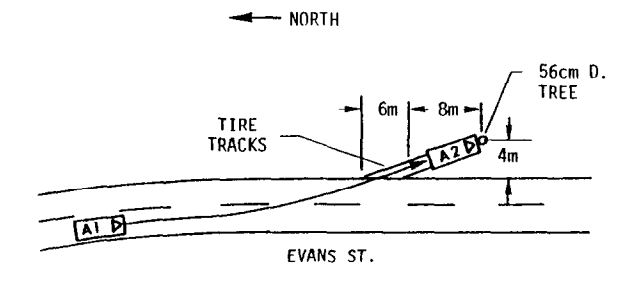


Figure 3. Occupant Injuries (Case No. 1).



Schematic of Accident Scene Figure 4. (Case No. 2).

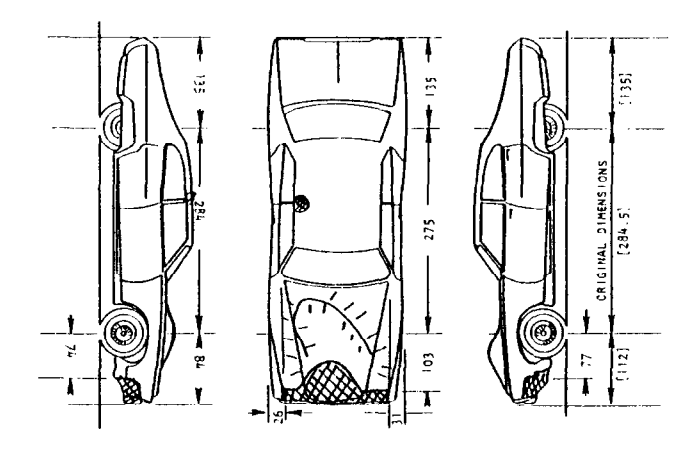
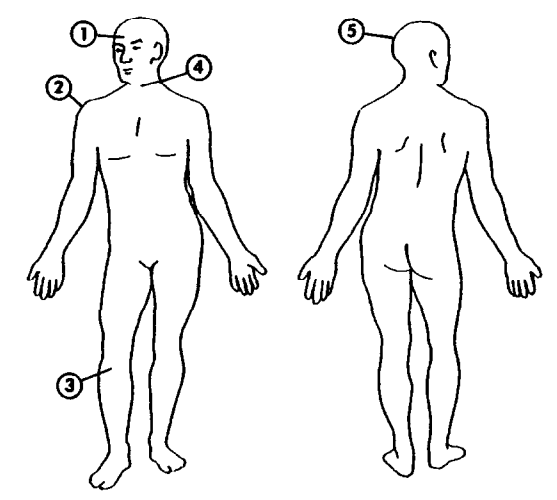


Figure 5. Vehicle Damage (Case No. 2).

- 1. Cont. and Abr. Forehead (2)\* 4. Cont. Larynx (2)
- 2. Cont. Rt. Shoulder (1) 5. Briefly Unconscious (2) 3. Lac./Abr. Below Rt. Knee (1)



\*Number in parenthesis is the estimated AIS number.

1. Multiple Fxs. Rt. Radius (2) 3. Fx. Rt. Acetabulum (2) 2. Fxs. 8,9 Lt. Ribs (1) 4. Fx. Rt. Tibia into Joint (3)

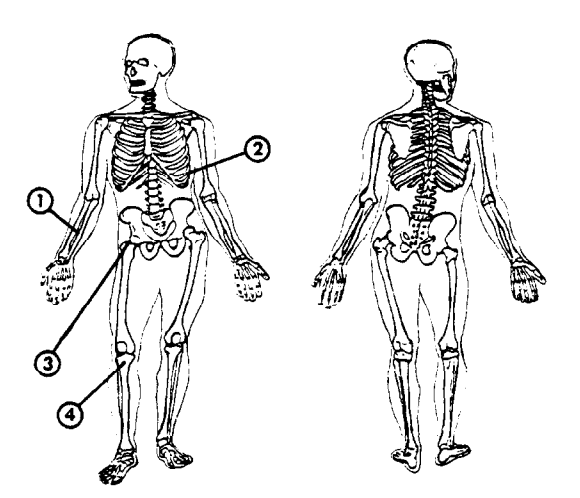


Figure 6. Occupant Injuries (Case No. 2).

to the head, neck, rib cage, hip, lower legs, and lower arms as detailed in Figure 6.

Use of CRASH II program yielded a velocity change of 28.6 mph (46.0 km/hr) along the axis of the Oldsmobile. This was represented as an acceleration in the form of a sine curve with a total duration of 80 ms.

CASE NO. 3: 1980 VOLKSWAGEN RABBIT (FRONTAL IMPACT, PASSIVE RESTRAINT) - A 1980 Volkswagen Rabbit, moving on a two-lane road, was struck by a Chevrolet Blazer that had crossed the centerline on an icy turn. The impact energy transfer was nearly "head-on" for the Rabbit. Schematics of the accident scene and the damage to the vehicle are shown in Figures 7 and 8.

The male driver was restrained by a passive belt system. Upon impact he continued forward against the shoulder belt and his knees contacted the knee bolster. He stated that he braced himself by straightening both legs and slamming both feet against the floorpan.

The fairly extensive damage to the car interior was concentrated in the left-front corner of the passenger compartment. The left end of the instrument panel was partially separated from the deformed left A-pillar. The steering wheel rim was slightly deformed by the driver who apparently braced his hands against it. There was some evidence of steering column movement to the left and slightly upward. The interior of the left door was deformed and the glass

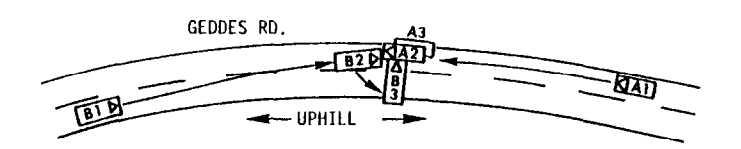


Figure 7. Schematic of Accident Scene (Case No. 10).

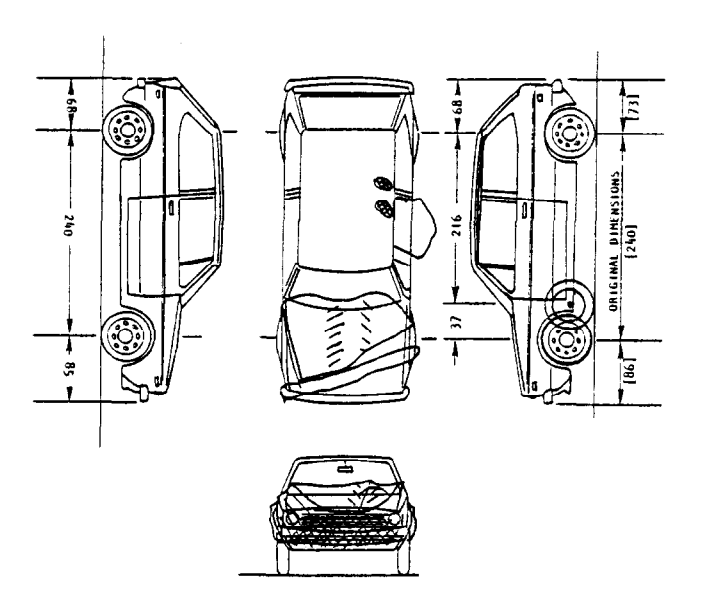
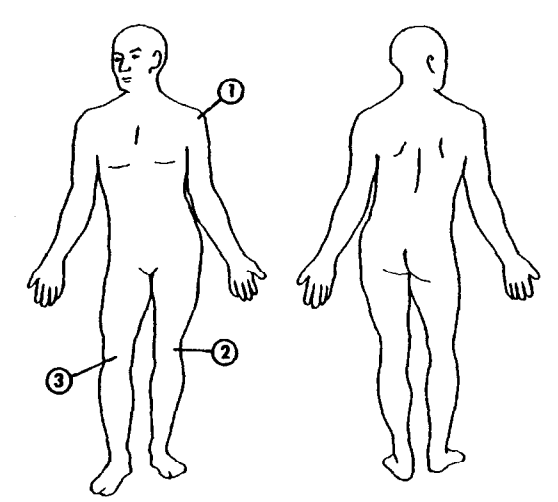


Figure 8. Vehicle Damage (Case No. 3).

- Cont. Left Shoulder (1)
   Partial tear Lt. Posterior Cruciate Ligament (3)
- Tear, Rt. Anterior Cruciate Ligament (3)



\*Number in parenthesis is the estimated AIS number.

 Split Fx. Rt. Tibial Plateau, Crushing Lateral Plateau, Avulsion Tibial Spine (3)

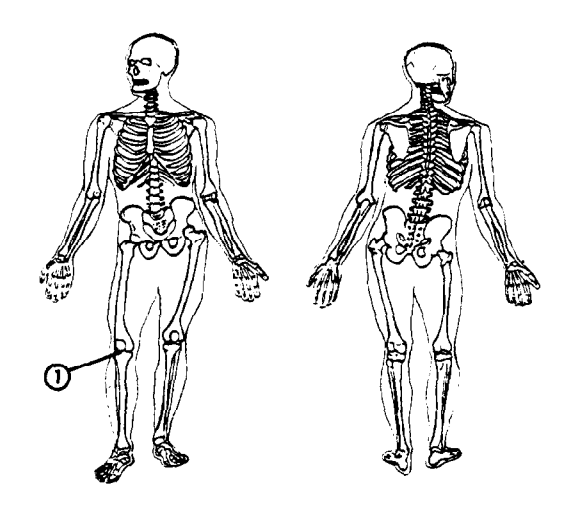


Figure 9. Occupant Injuries (Case No. 3).

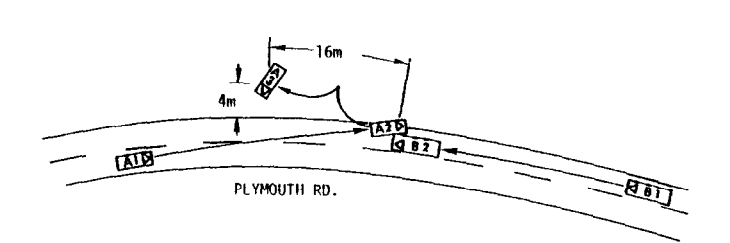


Figure 10. Schematic of Accident Scene (Case No. 4).

broken out due to impact but it is unknown if there was contact by the driver. There was intrusion of the instrument panel which forced the knee bolster back toward the driver's knees. The floorpan was buckled and the driver's seat adjuster deformed. The instrument panel around the instrument cluster was damaged and the damaged rearview mirror was dislodged from the severely crazed windshield, but it is unknown if there was any occupant contact.

The driver sustained only a contusion on the left shoulder due to the restraining force of the shoulder belt but suffered relatively severe knee injuries. The details are presented in Figure 9.

Use of the CRASH II program yielded a velocity change of 36.7 mph (59.1 km/hr) along the axis of the Volkswagen. This was represented as an acceleration in the form of a trapezoid with a total duration of 80 milliseconds and rise and decay times of 10 milliseconds.

1980 CHEVROLET CHEVETTE CASE NO. 4: (LATERAL IMPACT) - A 1980 Chevrolet Chevette was struck in the right side by a C-20 Chevy Van on a snow covered and slippery road. Intrusion was extensive on the passenger's side. The female driver of the Chevette was wearing a lapshoulder belt and sustained minimal injuries. Schematics of the accident scene and damage to the Chevette are shown in Figures 10 and 11. Although the subject vehicle spunout, it appeared that the primary force vector was lateral as judged by the exterior damage. Based on the assumed lateral force vector, it was decided to attempt simulation of this case also using the MVMA 2-D occupant motion simulation.

The lone female driver was wearing the 3-point restraint system. Upon impact she flexed to the right contacting the floor-mounted shift lever and right front door.

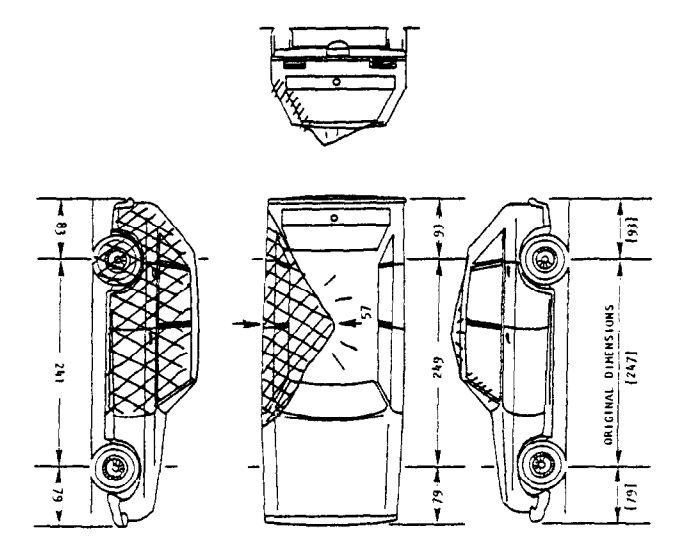
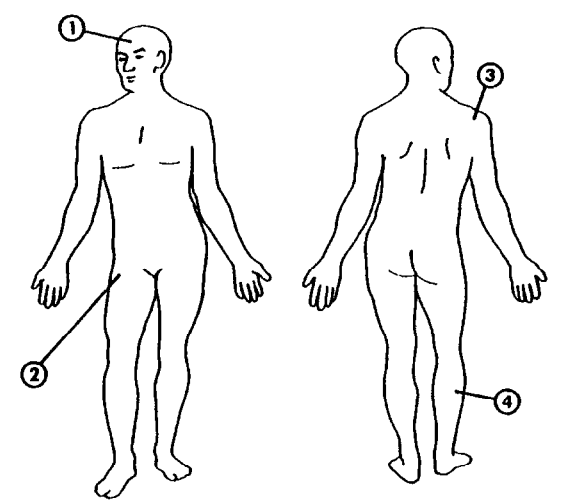


Figure 11. Vehicle Damage (Case No. 4).

- 1. Lac. Rt. Frontal Scalp (1)\* 2. Cont. Rt. Proximal Anterior and Medial Thigh (1)
- Lac. Posterior Rt. Shoulder (1)
   Cont. Rt. Calf (1)



\*Number in parenthesis is the estimated AIS number.

Figure 12. Occupant Injuries (Case No. 4).



Figure 13. Example of Driver in Normal Driving Position.

Damage was extensive to the right side of the passenger compartment. The floor-mounted Tbar shift lever was bent to the right by driver contact causing its plastic housing to crack. Deformation of the right upper A-pillar crazed the right half of the windshield, deformed the header, bowed the right sunvisor and deformed the roof in the right front corner. The right front door intruded about 41 cm (16.14 in.) damaging its latch housing, the front right seat cushion, and seat adjuster. Its window sill was also contacted by the driver. The right Bpillar intruded about 46 cm (18.11 in.) damaging the right front seat back and causing it to bend to the left behind the driver's seat back. Impact to of the right roof side rail deformed the roof.

The driver sustained only minimal injuries as illustrated in Figure 12. These were apparently due to contacts with the right door, Tbar shift lever, and seat belt buckle.

Use of the CRASH II program yielded a lateral velocity change of 35 mph (56.3 km/hr). This was represented as an acceleration in the form of a trapezoid with a total duration of 60 milliseconds and rise and decay times of 5 milliseconds based on an estimate of the amount of time for the impacting vehicle to cause the intrusion and transfer its motion.

## SPECIFICATION OF OCCUPANT POSITION

The first step in reconstruction of occupant dynamics using the MVMA 2-D occupant motion simulation was to develop an estimate of vehicle geometry and location of the driver within the vehicle. The key information used were engineering drawings of the vehicle, simple geometric measurements of the vehicle, plus information gathered during an interview with the driver when possible. During the interview simple anthropometric measurements were made documenting occupant size as shown in Table 1.

To develop the estimate of the posture of the occupant in the vehicle, photographs were taken showing normal driving position in a car essentially geometrically identical to the one involved in the crash. Figure 13 is an example photograph. A schematic of the vehicle interior cross-section was then made for a plane through the center-line of the occupant using vehicle scale drawings. The photographic slide of the

Table 1. Occupant Size

Case No.	Age	Stature		Weight		Sitting Ht.		Knee to Buttock Lth	
		ln.	(Cm.)	Lb.	(Kg.)	ln.	(Cm.)	In.	(Cm.)
1	35 (M)	72.2	(183.5)	20.05	(91.1)	39.1	(99.4)	24.1	(61.2)
2	50 (M)	69.2	(175.8)	182	(82.7)	37.2	(94.4)		
3	47 (M)	69.6	(176.7)	184	(83.6)	35-3	(89.7)		
4	21(F)	66	(167.6)	125	(56.8)				

seated occupant was then projected onto the schematic taking into account, insofar as possible, distortions based on camera placement. An outline of the occupant was then sketched onto the schematic (Figure 14). A linkage for the occupant was then superimposed using the anthropometry of the driver. The dimensions of the linkage were obtained by scaling known 50 percentile data to fit the four basic measurements which were made. The various contact surfaces defining the car interior are also identified for the case shown in Figure 14. Because of the lack of force-deflection data for the specific vehicles studies and the exploratory nature of the project, engineering estimates based on available information were used for these quantities.

## PREDICTED KINEMATIC AND DYNAMIC RECONSTRUCTIONS

Two types of displays are presented in this section to document the predicted kinematic and dynamic results. The first is a set of figures (15-18) showing occupant position as a function of time. Each figure contains a sequence of tracings of occupant position within the vehicle. The time points in the sequence have been selected to illustrate features of the occupant/vehicle interactions. Table 2 contains a summary of a selection of dynamic results.

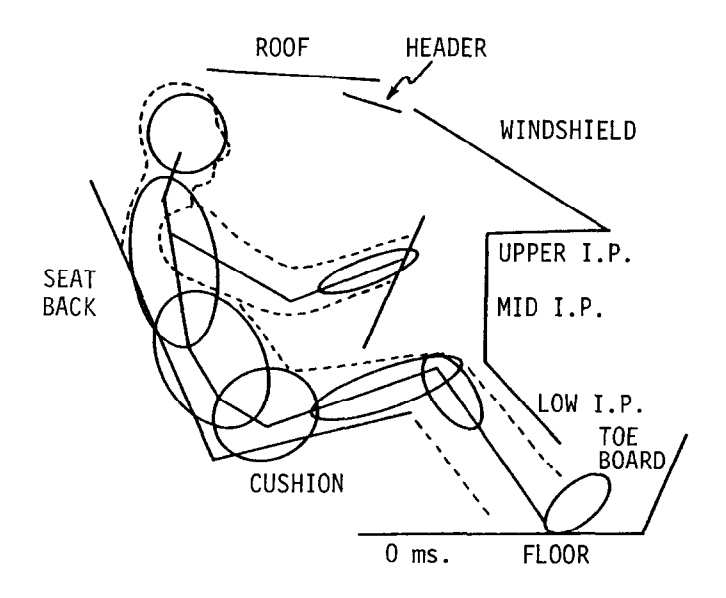


Figure 14. Subject and Reconstruction (Case No. 9).

Table 2. Predicted Peak Loads Applied to Occupant

Case No.	Body Segment	Vehicle Component	Contact Begins ms.	Contact Ends ms.	Peak Force	Peak G's
1	Head	Header	72	82	1900	114
1	Head	Windshield	95	108	1800	90
1	Chest	Steering Wheel	90	148	1800	4.5
1	Abdomen	Steering Wheel	82	115	400	
1	Femur	Instrument Panel	35	95	2600	
1	Tibia	Instrument Panel	38	95	1900	
2	Head	Header	60	65	400	41
2	Head	Windshield	70	80+	1600	15
2	Head	Instrument Panel	90	120	500	8
2	Chest	Steering Wheel	55	145	1150	5
2	Abdomen	Steering Wheel	35	85	300	
2	Femur	Instrument Panel	50	85	3100	
2	Tibia	Instrument Panel	48	85	1800	
3	Forearm	Steering Wheel	25	35+	1400	
3	Chest	Torso Belt	30	95	2600	5
3	Tibia	Bolster (N)	20	95	4000	
3	Tibia	Bolster (T)	20	95	1900	
4	Head	Window	73	77	1350	14
4	Belt	Pelvis	20	100	2300	
4	Arm/Shoulder	Door	60	70	1200	8
4	Rt. Upper Leg	Trans. Housing	25	65	1900	
4	Rt. Upper Leg	Trans. Housing	85	115	1000	
4	Leg	Shift Lever	35	60	1400	

Occupant/vehicle interactions are identified by body segment and vehicle component. The time for beginning and ending the dynamic event is noted as well as the peak force developed during contact. For body segments with automatic printout of G-levels, peak values are indicated.

CASE NO. 1 - Figure 15 shows a sequence of tracings of the simulated occupant positions for several points in time during the simulation. The first shows the initial position at 0 milliseconds. At 70 milliseconds the subject has moved forward and shows substantial contact with the lower instrument panel while contact with the header has just begun. The next tracing shows compression of the neck, resulting from the header contact and initiation of column/ thorax interactions. At 110 milliseconds the head rotates over the column and into the windshield. It is possible that the larynx contact may have occurred at this point or possibly later during the contact with the upper instrument panel shown in the final tracing. By 140 milliseconds the column/rim combination has compressed several inches in the simulation. approximates the deformations observed in the case vehicle. It should also be noted that by

140 milliseconds the knees and tibias are no longer interacting with the lower instrument panel. This represents the beginning of the rebound phase with the remainder of the body following during the remaining phases of the simulation.

Table 2 shows a summary of the dynamic output results produced by the simulation. The sequence of contacts of the head, first with the header, and then with the windshield, should be noted. As the occupant moves forward, the interaction with the steering column occurs first in the abdominal region followed by the interactions with the chest. Substantial normal forces are generated on both the femur (at the knee) and the tibia (just below the knee) during their contact with the lower portion of the instrument panel. Because of the two-dimensional nature of the MVMA 2-D occupant motion simulation, the numbers shown represent the sum of the loadings to both legs. Vehicle/occupant interactions observed as actual contact points in the crashed vehicle indicate that this assumption is

CASE NO. 2 - Figure 16 shows tracings of occupant position for several points in time

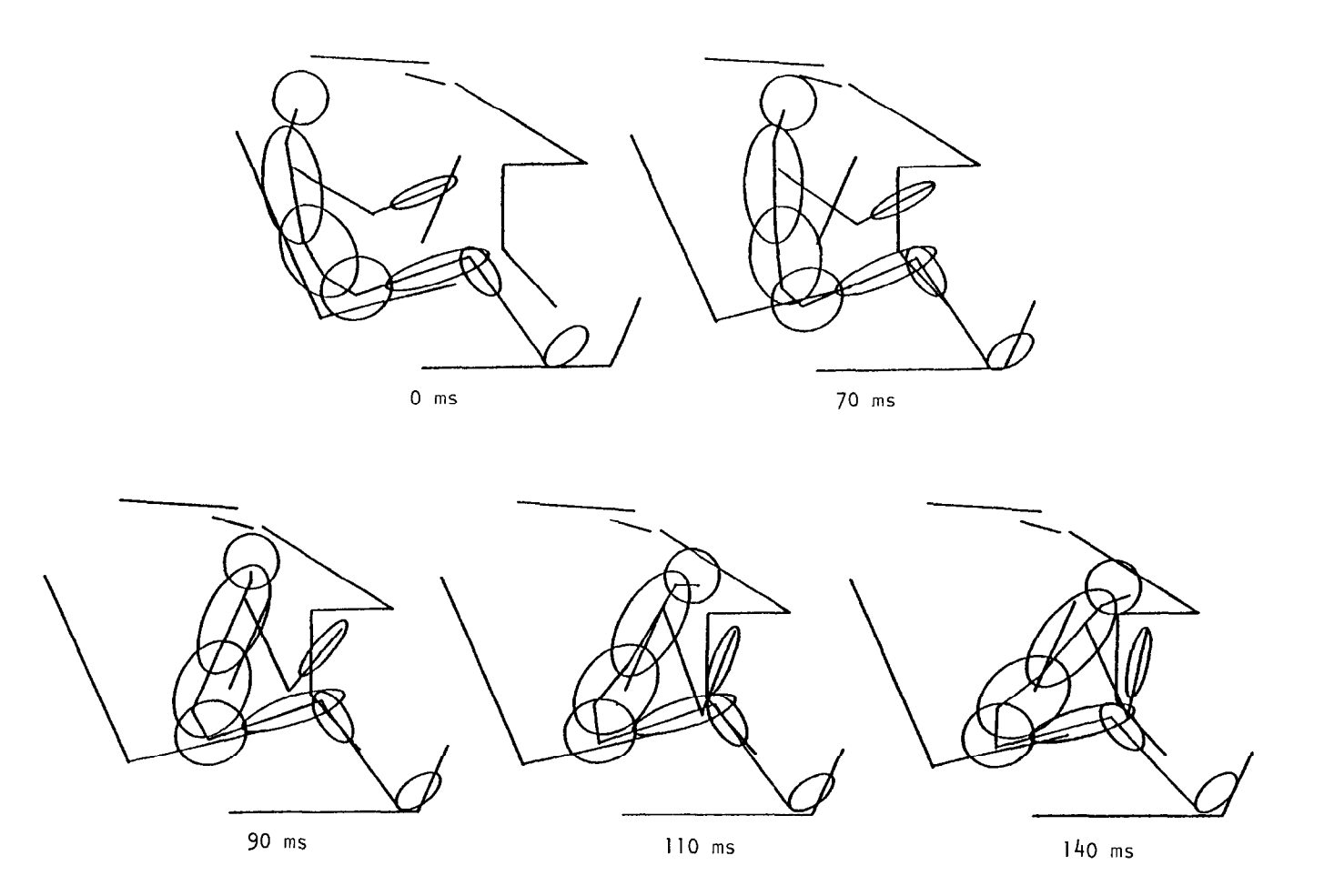


Figure 15. Sequence of Occupant Positions (Case No. 1).

during the simulation. The second tracing shows the beginning of knee/tibia interactions with the lower instrument panel at about 50 ms. Also, the abdomen is just beginning to contact the lower rim of the steering wheel. The next tracing at 60 milliseconds shows several interactions imminent or just beginning. The lower rim of the steering wheel is interacting with the lower region of the chest contact ellipse. At the same time the lower arm has moved forward and has penetrated the planes of the instrument panel. (No contacts were allowed for this segin the simulation, however this view represents a plausible location for the arm/ panel interactions documented in the accident reconstruction.) At this point in time, the head is just about ready for a contact with the header. It was necessary to add a small circle to the top of the head (shown in the tracings) in order to sense this contact due to the short length of the header, the relatively large size of the main head ellipse, and the relatively small penetration of the head into the header. The next tracing shows the primary interaction with the windshield while the last tracing shows the predicted position of most forward excursion with the head and neck contacting the steering wheel rim and the instrument panel. It should be noted that rebound has been initiated by 100 milliseconds in the areas of the lower extremities. This rebound is transmitted on up the linkage as the simulation continues.

Table 2 summarizes some of the dynamic output results produced by the simulation. first three interactions involve the head with the header, windshield, and instrument panel. The end of head/windshield contact is listed as 80+ to indicate low force contact as the head slides down after the initial impact. The head and chest accelerations are, as in Case No. 1, well correlated with the phasing of the loadings. The head G-loading, due to the header contact, is relatively low. This is a case where small changes in input data could dramatically change the simulation. If the occupant sat 1/2 inch lower (1.27 cm), the contact would not occur. If he were 1/2 inch (1.27 cm) higher, the size of the force spike would likely be larger than that for the windshield. The effect of vehicle pitch during the tree impact was not investigated due to the limited nature of the project and could also be a major factor in

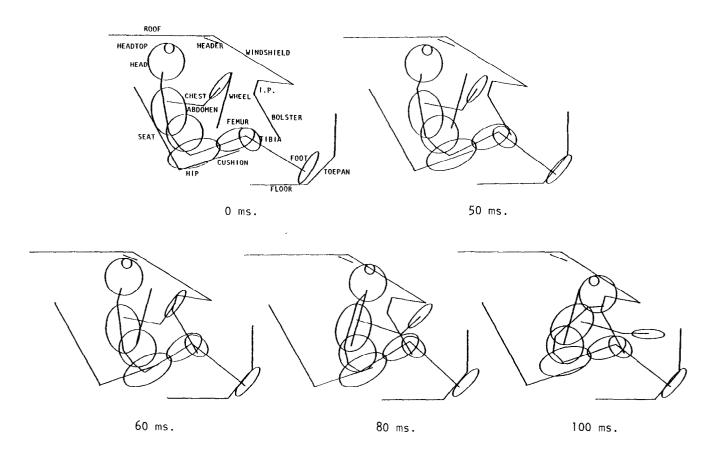


Figure 16. Sequence of Occupant Positions (Case No. 2).

the relative position of the head with respect to the vehicle in the timing of this contact. Interactions of the chest and abdomen with the steering wheel/column are listed next in Table 2. The abdomen is in contact for approximately 20 ms before the rib cage becomes substantially involved in the dynamics. The tibia and femur loads show the considerable force which was likely transmitted to the acetabulum.

CASE NO. 3 - Figure 17 shows tracings of the simulated occupant positions for several points in time during the impact. The tibia was in contact with the knee bolster by 30 milliseconds. At 60 milliseconds, the occupant shows the beginnings of effects due to the upper torso restraint. The next tracing shows the farthest forward excursions of the body with the beginnings of rebound in the lower legs. The location of the arms and hands throughout the sequence should also be noted. The final tracing shows complete rebound at a time of 160 milliseconds.

Table 2 shows some of the dynamic output results produced by the simulations. Interactions between the forearm and the steering wheel are listed first. Although the magnitude of the initial spike is probably unrealistic from a

human response point of view, the ability to feed force and energy into the body through this part of the linkage in a relatively continuous manner has been demonstrated. The end of contact is listed as 35+ to indicate very low for-Redefinition of the ces after that point. force-deflection curve for the steering column which was used for this simulation, to reflect a softer material property for wheel rim deformation, would probably solve much of the problem. Similarly, the properties of elbow and shoulder joints could be refined to include muscle tension effects and the mobility of the shoulder girdle. No well-researched data have been developed to this point in time for definition of shoulder girdle mobility. The next entry in Table 2 shows the major restraint effect on the chest due to the upper torso belt. The final entries show the normal and tangential forces on the tibia due to contact with the bolster. This force is transmitted into the knee joints as a shear force. The intrusion of the knee bolster into the occupant compartment was not explored in the analysis although it was observed in the This intrusion could have had a crashed car. marked effect on the results. Although not presented in Table 2, the timing of peak head

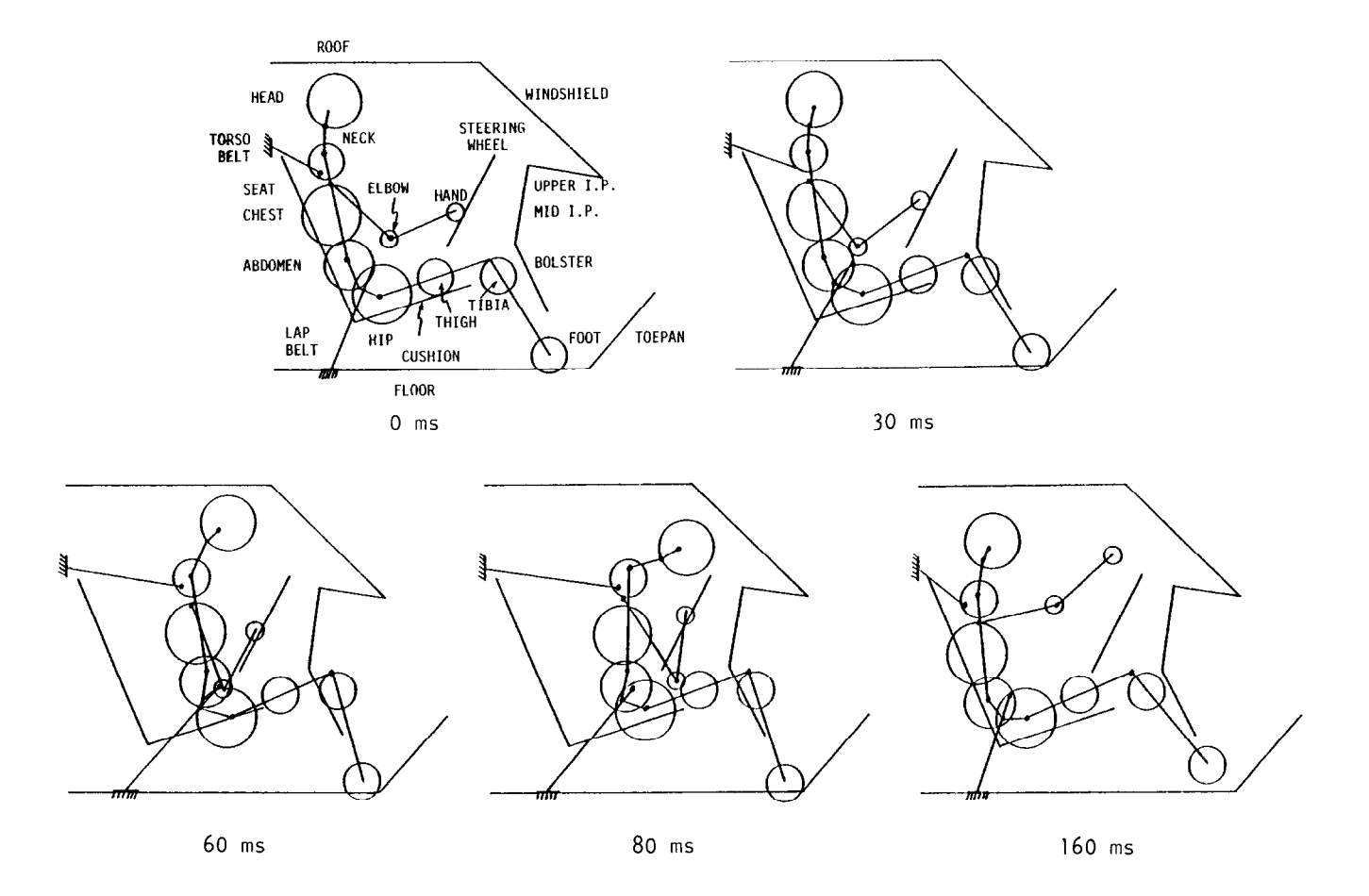


Figure 17. Sequence of Occupant Positions (Case No. 3).

accelerations follow the peak chest accelerations which appears to be directly related to the application of the belt forces. This phasing relation is related to the pitching down of the head with respect to the upper torso. There is no evidence of contact of the head with the car interior.

CASE NO. 4 - Figure 18 shows tracings of the simulated driver's position for several points in time during the impact. The occupant linkage concept for using the MVMA 2-D occupant in case of side impact was motion model developed by Robbins and Becker (2). By 40 milliseconds the legs and torso have contacted the transmission housing and/or the shifter. The belt is just beginning to exert force. (It has been assumed that the driver slipped from under the upper torso portion of the 3-point belt system). Also, she is just beginning to pivot down toward the intruded door. At 60 milliseconds the driver has pivoted toward the door. The arm has just initiated contact which will peak in about 10 milliseconds. The belt is effectively restraining the torso from riding over the transmission housing. The next tracing shows the occupant at 80 milliseconds. The torso has pitched over completely and the head has contacted the window in the sill region. By the

end of the simulation the subject has rebounded showing the effects of the belts.

Table 2 shows some of the dynamic output results produced by the simulations. The first entry shows the force on the head produced during the window sill region contact. The restraining effect of the belt is shown next. The effect of the belts is to prevent the lower torso and extremities from completely riding over the transmission housing. The arm/shoulder interaction with the door follows. Computer exercises using either more or less passenger compartment deformation resulted in higher or lower force of interaction. The next two entries document the interaction of the thighs and upper legs at the hip with the transmission housing. The location of the 3-point belt stalk near the housing and the minor injury suffered by the driver most likely resulted from this interaction. The interaction between the leg and shift lever is listed last. It is predicted to occur early in the dynamic event. In most cases body acceleration peaks correlate well with observed kinematic or dynamic events. Chest accelerations shift from lateral (40-60 milliseconds) to vertical (60-80 milliseconds) as the belt system and shift housing causes the torso to pitch toward the side. A clean spike shows up in the

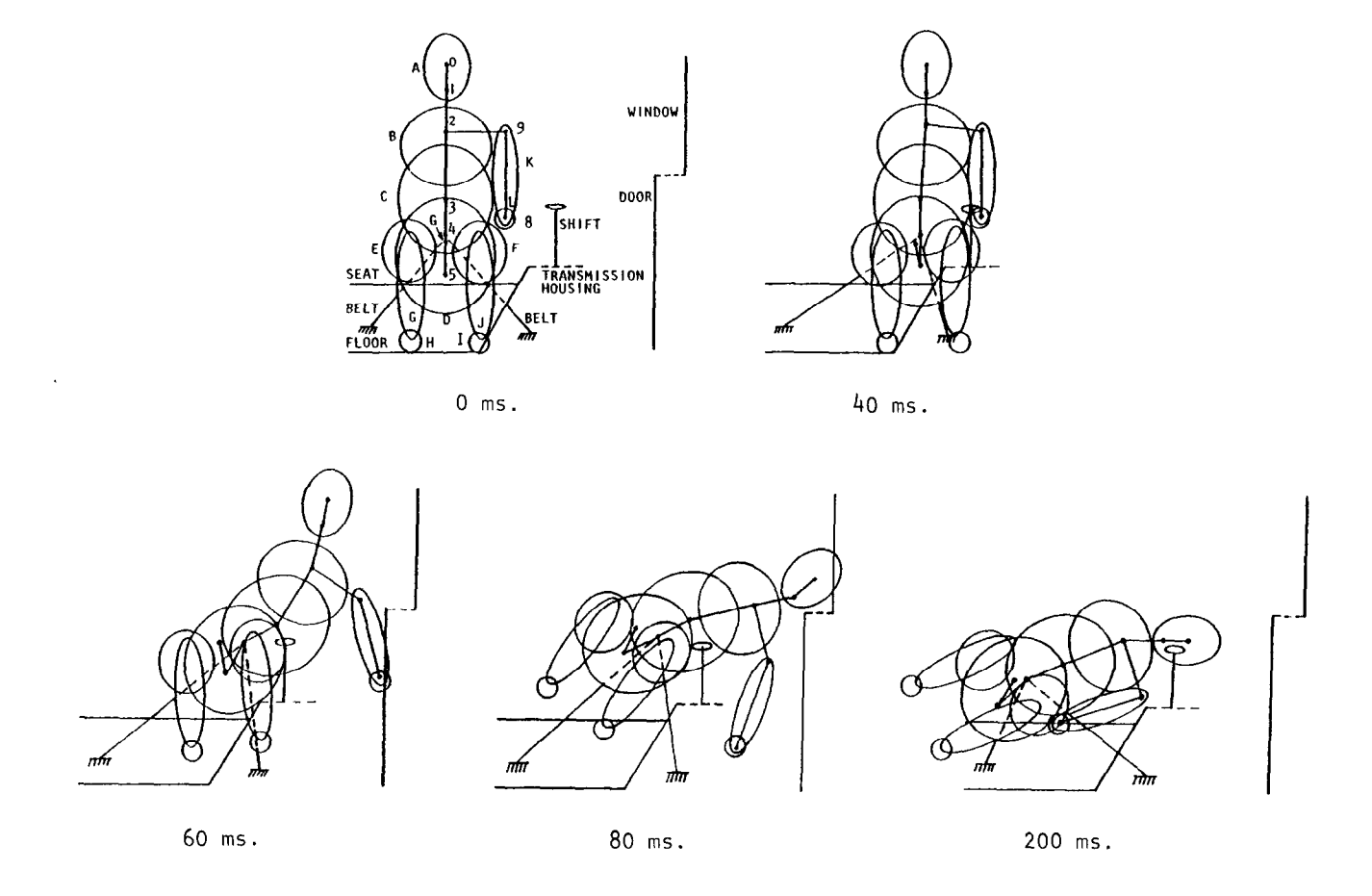


Figure 18. Sequence of Occupant Positions (Case No. 4).

head lateral acceleration which correlates well with the interaction in the window sill region.

## BIOMECHANICAL REVIEW OF RECONSTRUCTIONS

This section discusses the biomechanical aspects of the four reconstructions in terms of the accelerations of body regions, contact forces and resulting injuries. Comparisons are made between the results of the various reconstructions to highlight differences and similarities.

CASE NO. 1 - This large, 35-year-old male sustained significant head impacts against the header and windshield. The force levels of 1800 to 1900 lbs., associated with these impacts, would not be expected to cause frontal bone skull fractures although they approach the lower limits of frontal fracture tolerance for flat impact surfaces (3). Similarly, the head accelerations associated with these two impacts are moderately severe (peaks near 120 G's). Additional head acceleration peaks around 90 G's are also present, and the entire head acceleration-time history is characterized by significant time durations as well as acceleration magnitudes. This driver was concussed for 2 to 3 minutes.

The size and position of the driver and the vehicle interior geometry combined to produce a uniform contact of the chest squarely with the steering wheel. Although uniform, the loading was severe enough to fracture the sternum. The predicted load peak was approximately 1800 lbs. which is similar in magnitude to those produced by experimental studies on chest impact with cadavers (4). The peak chest accelerations associated with the impact were less than 50 G.

The contact of the driver's legs with the instrument panel produced an average force of 1300 lbs. in each femur and 950 lbs. into each lower leg beneath the knee. This resulted in a total femur load of approximately 2250 lbs. in each leg as the lower leg force would be transmitted by shear to the upper leg. The lower leg load was close to tolerable values for knee joint ligamentous damage in cadavers (5). The driver was tall and had robust legs. Neither the average lower leg loads of 950 lbs. nor the total femur loads of 2250 lbs. were likely near the tolerance of this driver (6).

The most severe injury sustained by the driver was a possible fractured larynx which has an AIS rating of 4. However, the forces and accelerations generated in the head and chest impacts, and the initiation of temporary brain dysfunction and chest structural damage, are indicative that the thresholds of severe injury for the driver's head and chest were being approached in this crash.

CASE NO. 2 - This case involves a more severe frontal crash than in Case 1 (28.6 mph versus 22.9 mph) with an older, smaller male driver (50 years old) of a larger car. The contact of the head with the header was not as severe as the windshield contact, which produced a peak of 1600 lbs-well below frontal bone

fracture tolerance (3). The head acceleration associated with the windshield contact was higher than that of Case 1 (150 G peak) but with a lesser duration. Similar longer duration acceleration peaks around 80 G occurred late in both crashes. The driver was only briefly unconscious.

The contact of the driver's chest with the steering wheel was not as uniform or aligned as in Case I due to configurational differences in the vehicle interior and his pre-crash positioning. A peak chest load of 1150 lbs. was produced. The fractures of the 8th and 9th ribs on the left side may have been due to the interaction of the bottom half of the steering wheel. The age of the driver may also have had an influence on the production of skeletal damage at the lower load of 1150 lbs. Despite the lower load, the peak chest accelerations were slightly higher (50 G) than in Case 1.

The average femur contact force was 1550 lb. on each knee. The average tibial force was 900 lb. per leg and the total average femur load would be 2450 lb. per leg. The deformation of the instrument panel due to knee contact was greater on the left side and may have contributed to more of the load being carried by the right leg. The fracture of the right tibia occurred with a predicted load of at least 900 lbs. Both the age and the lesser lower leg development of the driver may have also influenced the initiation of this fracture at loads successfully sustained in Case 1. The driver also sustained a fracture of the right acetabulum, again at a load of at least 2450 lbs. but most likely greater than that. Both of these load level ranges (900 to 1800 lbs. and 2450 to 4900 lbs.) are consistent with the tolerance limits derived from cadaver leg impacts (5,6).

CASE NO. 3 - Unlike the previous two cases, this frontal crash involved a 47 year old driver using a passive belt restraint system and a much greater impact severity. Due to the upper torso restraint belt, the head acceleration-time history was quite different from those of the previous cases. It was less abrupt in nature and had no contact spikes, although the peak reached 100 G. The duration of the waveform was much greater than the other two cases. No loss of consciousness was noted.

The upper torso belt loads reach 2600 lbs. during the crash without skeletal damage. This value is significantly greater than cadaverbased limits of 1300 to 1500 lb for a minimum number of rib fractures due to belt loading (7).

The driver's lower leg location resulted in significant loading to the lower legs by contact with the knee bolster. The peak average force acting on each tibia was 2000 lbs., well above the level for ligamentous damage to cadaver knee joints (5). Both knee joints received ligament damage with the right tibial plateau sustaining a split fracture at these high load levels.

CASE NO. 4 - This was a severe far-side impact involving a female driver restrained by a 3-point belt system. The intrusion of the right

side of the vehicle provided a significant head contact point which produced an abrupt 1350 lb. peak force to the head. The contact resulted in a laceration to the right frontal scalp of the driver. The load peak was well below skull fracture tolerance for a flat surface impact to the frontal bone (3). The lateral head accelerations were low except for the abrupt contact spike with a peak of 140 G. The vertical head accelerations were equally as high but with much greater duration during this contact. The subject was not concussed.

A significant impact force (1200 lbs. peak) was produced by contact of the right shoulder with the intruded vehicle interior. There are no biomechanical shoulder force data to compare this with, however. This contact also produced very high chest accelerations although the realism of lateral shoulder response data for the model can not be validated at this time. Large loads were also predicted against the thigh (1900 lbs.) and lower leg (1400 lbs.) by interaction with interior components. No significant injuries were produced, however.

## CONCLUSIONS

- 1. A primary goal of this project was to combine state-of-the-art detailed accident investigation procedures, computerized car crash and occupant motion modeling, and biomechanical analysis of human injury causation, into a method for obtaining enhanced biomechanical data from vehicle crashes. This method involved organization of a multidisciplinary team which investigated and analytically reconstructed four accident cases. The reconstructions, using largely preliminary data, were evaluated and the dynamic loadings predicted for application to the vehicle occupants yielded injury results which were generally within accepted ranges of known tolerance data.
- 2. Vehicle trajectories and post-crash positions must be documented completely, insofar as is possible, to allow a reasonable prediction of velocity change during impact, and hence, to allow a reasonable approximation for car acceleration or position to be made as a function of time. Use of CRASH and SMAC programs are not reliable if this information is not available.
- 3. Improved force-deformation data for both vehicle components and the occupant would improve predictions of force and acceleration magnitudes, energy absorbed by segments of the human body, and as a result, the rebound.
- 4. The use of the interview of the injured vehicle occupant was very informative with respect to:
  - Details of the accident
  - His or her physical size
  - Estimated driving posture in a car at the time of the crash
- All subjects were very interested in the project and much more cooperative and useful than was originally estimated.
- A data bank on human anthropometry should be established for use in studies such as

this based on human dimensions, mass distribution, inertial properties, joint locations, joint mobility, and joint strength. Most of the data available to the project was based on definitions and measurements made on anthropomorphic test devices. These data were particularly suspect for neck and shoulder mobility, flexibility, and elongation.

6. The analytical methodology provides a technique for adjusting parameters as new data become available. For example, parameters, all required in the analytical reconstruction, could represent quantities relating to the vehicle dimensions, the accident definition, vehicle damage definitions, occupant physical and properties anthropometry, (strength, force-deformation) of the occupant or vehicle. In other words, a reconstruction is not lost after the first attempt. It can be improved upon either by the original team, or later by others with more complete data.

### REFERENCES

- B.M. Bowman, R.O. Bennett, and D.H. Robbins. "MVMA Two-Dimensional Crash Victim Simulation, Version 4." 3 vols., Report No. UM-HSRI-79-5. Ann Arbor: Highway Safety Research Institute, The University of Michigan, June 1979.
- D.H. Robbins and J.M. Becker. "Baseline Data for Describing Occupant Side Impacts and Pedestrian Front Impacts in Two Dimensions." Report No. UM-HSRI-81-29. Ann Arbor: Highway Safety Research Institute, The University of Michigan, June 1981.
- R.L. Stalnaker, J.W. Melvin, G.S. Nusholtz, N.M. Alem, and J.B. Benson. "Head Impact Response" SAE Paper No. 770921. Proceedings of the 21st Stapp Car Crash Conference, New Orleans, La., October 1977.
- C.K. Kroell, D.C. Schneider, and A.M. Nahum. "Impact Tolerance and Response of the Human Thorax" SAE Paper No. 710851. Proceedings of the 15th Stapp Car Crash Conference, San Diego, Cal., November 1971.
- Viano, C.C. Culver, R.C. Hout. J.W. Melvin, M. Bender, R.H. Culver, and R.S. Levine. "Bolster Impacts to the Knee and Tibia of Human Cadavers and an Anthropomorphic Dummy" Paper SAE No. 780896. Proceedings of the 22th Stapp Car Crash Conference, Ann Arbor, Mi., Conference, Ann Arbor, Mi., Oct. 1978.
- J.W. Melvin, R.L. Stalnaker, N.M. Alem, J.B. Benson, and D. Mohan. "Impact Response and Tolerance of the Lower Extremities" SAE Paper No. 751159. Proceedings of the 19th Stapp Car Crash Conference, San Diego, Cal., 1975.
- R.H. Eppinger. "Prediction of Thoracic Injury Using Measurable Experimental Parameters" Report on the 6th International Technical Conference on Experimental Safety Vehicles. U.S. Department of Transportation, Washington, D.C. Oct. 1976.